Anat Embryol (1988) 179:109–127

Anatomy
and Embryology

The rat inferior olive as seen with immunostaining for glutamate decarboxylase

Barbara J. Nelson and Enrico Mugnaini
Laboratory of Neuromorphology, Box U-154, The University of Connecticut, Storrs, CT 06268, USA

Summary. Boutons presumed to use γ-aminobutyric acid as neurotransmitter (GABAergic boutons) were detected by glutamate decarboxylase (GAD) immunocytochemistry in all regions of the rat inferior olive. The remarkably high concentration of these boutons allowed a clear visualization of olivary subnuclei boundaries. Regional variations in GAD immunostaining intensity were observed within the nuclear complex and were graded both visually and photometrically. The regional staining variations, for the most part, followed subnuclei boundaries and olivary zonal compartments that have been delineated by the topography of climbing fiber projections. Some subnuclei were grouped by similar staining intensities. The beta nucleus and a medial region in the ventral fold of the dorsal accessory olive were most intensely immunostained, followed by the subnucleus c of the medial accessory olive. Lower staining intensities were observed in the dorsomedial cell column, the dorsal fold of the dorsal accessory olive and the dorsal cap. The lowest intensities were observed in the subnuclei a and b of the medial accessory olive, the ventrolateral outgrowth, the rostral lamella of the medial accessory olive, the principal olive, and the lateral part of the ventral fold of the dorsal accessory olive. The factors contributing to the variations in immunostaining intensity (bouton size and frequency of occurrence) were investigated. The largest boutons were observed in the beta nucleus. Intermediate sized boutons were observed in the dorsomedial cell column, dorsal cap and the dorsal fold of the dorsal accessory olive. The smallest boutons were present in the remaining regions of the inferior olive, including the principal olive, the rostral lamella of the medial accessory olive, and the ventral fold of the dorsal accessory olive. The medial region of the dorsal accessory olive ventral fold contained a higher density of GABAergic boutons than other regions. GABAergic bouton size and innervation density therefore largely accounted for the variations in GAD immunostaining intensity. This study provides a map of the rat inferior olive based on the distribution of GABAergic nerve terminals, and may serve as a basis for characterizing different GABAergic afferent systems in the inferior olive.

Key words: Rat – Inferior olive – GABA – Glutamate decarboxylase – Cerebellar circuitry

Offprint requests to: B.J. Nelson

Abbreviations: aMAO, subnucleus a of MAO; *bMAO,* subnucleus b of MAO; *beta,* subnucleus beta; *cMAO,* subnucleus c of MAO; *DAO,* dorsal accessory olive; *dc,* dorsal cap; *dfDAO,* dorsal fold of DAO; *dl,* dorsal lamella of PO; *dlPO,* dorsal lamella of PO; *dmcc,* dorsomedial cell column; *lat vfDAO,* lateral portion of ventral fold of DAO; *MAO,* medial accessory olive; *med vfDAO,* medial portion of ventral fold of DAO; *PO,* principal olive; *rMAO,* rostral lamella of MAO; *vfDAO,* ventral fold of DAO; *vl,* ventral lamella of PO; *vlPO,* ventral lamella of PO; *vlo,* ventrolateral outgrowth; *GABA,* gamma-aminobutyric acid; *GAD,* glutamate decarboxylase

Introduction

The inferior olive (IO) is a nuclear complex which is present in all vertebrates, albeit in varying form (Whitworth and Haines 1986). Among all precerebellar nuclei, it is the only one that provides afferents to the entire cerebellum (Campbell and Armstrong 1983a). The IO is the major and probably the only source of climbing fiber afferents (Courville and Faraco-Cantin 1978; Desclin 1974; Szentágothai and Rajkovitz 1959). Climbing fiber activation produces a direct excitation of the Purkinje cell, bypassing the granule cell linkage used by the mossy fiber system (Eccles et al. 1967; Ito 1984). Unlike climbing fibers, the mossy fibers originate from a large number of brainstem and spinal cord sources (reviewed by Bloedel and Courville 1981). Although climbing fibers are pancerebellar, the IO receives afferents from about twenty neural centers. These projections terminate in distinct, although largely overlapping, regions of the IO (Brown et al. 1977; Swenson and Castro 1983; Walberg 1956, 1960; review of Martin et al. 1980). Their transmitter substances and effects on olivary activity have only partly been explored.

Some years ago, glutamate decarboxylase (GAD, EC 4.1.1.15), the synthetic enzyme for the amino acid neurotransmitter gamma-aminobutyric acid (GABA), was purified and antibodies were produced against it (Oertel et al. 1981a; Wu et al. 1973; Wu 1976). It therefore became possible to localize presumed GABAergic elements in brain with immunocytochemical procedures (McLaughlin et al. 1974; Mugnaini and Oertel 1985; Oertel et al. 1981b, 1982, 1983; Roberts 1979; Saito et al. 1974; Wood et al. 1976). Immunocytochemistry detects GAD exclusively in neurons presumed to be GABAergic and inhibitory (review of Krnjević 1976; Mugnaini and Oertel 1985). This conclusion has recently been strengthened by the corresponding localization of immunoreactivity to antibodies produced against

GABA-glutaraldehyde conjugates (reviewed by Ottersen and Storm-Mathisen 1987). It is possible, therefore, to reliably explore GABAergic projections to the IO with the purpose of morphologically distinguishing its inhibitory inputs.

During extensive immunocytochemical studies on the mode of distribution of brain GAD in mammals (Mugnaini et al. 1982; Mugnaini and Oertel 1985), we became impressed by the regional variations in immunostaining and by the high density of GABAergic axon terminals in the entire IO complex. (See also Gotow and Sotelo 1987; Sotelo et al. 1986). This mode of distribution contrasts with the discontinuous distribution of other neurochemical substances associated with olivary afferents (see Marani 1986 and Paré et al. 1987 for references). Projections from the IO to the cerebellar cortex and to the cerebellar nuclei are topographically organized, and connected regions of the cerebellar cortex, the IO and the cerebellar nuclei have been thought of as representing separate functional units (reviewed by Voogd and Bigaré 1980). Variations in GAD immunostaining intensity may correspond to differences in the amount of GABA synthesized and released at the synapse. Yet, since GABAergic boutons are present throughout the entire IO, GABA may have a universal role in modulating the activity of climbing fibers. Therefore, a detailed study of the GABAergic innervation of the inferior olivary complex seemed compelling.

In this paper we will describe the GABAergic innervation of the IO in rat. This laboratory animal is widely used in neuroanatomy, and lends itself to experimental studies requiring a large number of specimens. The comparative aspects and the origins of the GABAergic innervation of the IO will be presented in subsequent publications. Some of the results have been published in abstract and review form (Mugnaini et al. 1982; Nelson et al. 1984, 1986; Nelson and Mugnaini 1985, 1988) and have been presented in an unpublished overview lecture (Soc. Neuroscience, Dallas 1985).

Materials and methods

The results were obtained from sixteen adult Sprague-Dawley rats, weighing 150–300 g. Under deep pentobarbital anesthesia, the rats were perfused transcardially with a saline vascular rinse, followed by a zinc-aldehyde fixative, pH 4.5 (Mugnaini and Dahl 1983). This fixation procedure produces optimal immunostaining of axonal boutons. After fixation, the brains were dissected out, cryoprotected in a 30% sucrose and 0.9% NaCl solution, and sectioned at the 20–25 μm setting on a freezing microtome.

The brainstems of 9 rats were cut coronally, and sections through the IO were collected for immunostaining at intervals of 100 μm. In four of these rats, adjacent sections were processed for Nissl staining with cresyl violet. The brainstems of 2 additional rats were also cut coronally, but in one case every section was immunostained, and in the other case alternate sections were Nissl stained or immunostained, thereby providing two complete coronal series of sections through the IO. The brainstems of 2 rats were cut in the horizontal plane, and every section through the dorso-ventral extent of the IO was immunostained. Three complete sagittal series were collected through the medial-lateral extent of the IO. Two of these series were immunostained for GAD, and one series was stained with cresyl violet.

Immunostaining procedure

Floating sections were immunoreacted for GAD visualization with a sheep antiserum raised against rat GAD produced by Oertel et al. (1981a). Tris-HCl (0.5 M and pH 7.6) was used throughout the procedure as a diluent of the immunoreagents and as a rinsing solution. Sections were incubated for one hour at room temperature in a blocking solution of 5% normal rabbit serum (Miles Scientific) and 0.25% Triton X-100. The sections were then directly transferred to a solution containing the GAD antiserum diluted 1:2000 and 1% normal rabbit serum, and incubated for 48–72 h at 4° C with continuous gentle agitation. After thorough rinsing in several changes of buffer for one hour, the sections were post-fixed for 15 min in 0.125% glutaraldehyde in buffer. After rinsing, the sections were incubated for 40 min at room temperature in a linking antiserum (rabbit anti-sheep IgG, Miles Scientific) diluted 1:50, rinsed for 30 min in buffer, and incubated for another 40 min in goat PAP (Sternberger-Meyer Immunocytochemicals) diluted 1:100. The linking antiserum and PAP solutions contained 1% normal rabbit serum. After rinsing in several changes of buffer for 30 min, incubation in the linking and PAP antisera was repeated (Ordronneau et al. 1981). DAB (0.05% in a 0.01% hydrogen peroxide solution) was used as chromogen. The sections were mounted in glycerol-phosphate buffer (3:1) medium, or were dry mounted in Permount (Fisher Scientific) for light microscopic analysis.

A series of sections from the IO of one rat was processed for semi-thin sectioning. The sections were immunoreacted following the procedure described above, with the modification that 0.025% Triton X-100 was added to the primary antibody solution. After immunostaining, sections were rinsed for one hour in three changes of 0.12 M phosphate buffer (pH 7.3) and fixed for 30 min in chilled 1% osmium tetroxide in 0.12 M phosphate buffer. After dehydration in a series of ethanols, sections were embedded in an Epon/TAAB resin mixture. Semi-thin sections, 2 μm thick, were obtained on an ultramicrotome, mounted on glass slides and coverslipped with embedding resin.

Analysis of immunostaining

Three methods were used to analyze GAD immunostaining of the rat IO:

1) Visual inspection. A drawing tube attached to a light microscope was used to trace the subdivision boundaries of the IO in Nissl stained and GAD-immunostained serial sections. Direct inspection in the light microscope was used to judge regional differences in GAD immunostaining intensity in the IO. These data are presented as a series of light photomicrographs of the IO (Figs. 1–6). Regional staining intensities were visually scored on a scale of 1 to 5, where 1 indicates the lowest intensity of staining.

2) Photometry. Values of immunostaining intensity were obtained with the light meter of a Nikon Microphot FX microscope and expressed as exposure time in seconds. (For use of this procedure in immunocytochemistry, see Takahashi et al. 1987.) The spot used to measure exposure time had a 20 μm diameter (1% of the total objective viewing field). Measurements were made at 80X total magnification with ASA setting of 12. The spot meter was positioned

over areas of the neuropil which lacked capillaries and large axon bundles. In order to compare exposure times obtained from different animals and different sections of the same animal, exposure times obtained in the immunonegative pyramidal tract were subtracted from the readings obtained in the IO. Five values from each region were averaged and are presented in Table 1. In order to facilitate comparisons among individuals, each mean exposure time was also expressed as a percent of the value obtained from the beta nucleus, since this was the most intensely stained region of the IO. These percent values were averaged across three individuals, and are illustrated in Fig. 7.

Some variation in photometrically determined intensity occurred in corresponding regions of different animals, presumably because the intensity of immunoreaction is affected by variables such as penetration of immunoreagents and actual section thickness. Therefore, when measurements relevant to site comparisons were made either in different sections from a single animal or in sections from different animals, sections were chosen that had similar background values.

3) Analysis of individual boutons. Plastic embedded GAD-immunostained sections, 2 μm thick, were used to analyze the individual sizes and the density of GABAergic boutons in various regions of the rat IO. Sections were photographed with a 100X, oil immersion objective lens. Photographs of eleven different regions of the IO were printed to a final magnification of 1880X. This method gave sharp images of bouton-like particles.

A magnifier with a micrometer scale was used to measure the long and short diameters of 30 immunostained puncta in each region. Only particles that appeared to be in focus and non-contiguous with other puncta were included in the study. The diameters were then converted to actual scale. Since the shapes of the puncta varied, the product of the long and short diameters was used as an approximate measure of "bouton area". The areas of 30 bouton-like particles were averaged for each region to obtain a "mean bouton area" and corresponding standard deviation. In order to identify which olivary regions contained puncta of unique sizes, a multiple comparison of mean bouton areas for eleven olivary regions was performed with the Ryan-Einot-Gabriel-Welsch multiple range test. All statistical analyses were performed with Statistical Analysis System software (SAS Institute Inc., Cary, North Carolina) on an IBM 370 computer.

The frequency of occurrence, or density, of GAD-positive puncta was determined for eleven regions in the IO. Density was obtained by counting puncta in a 400 μm^2 area, and six measures were averaged per region to obtain the mean bouton density per unit area of a region.

Results

Parcellation of IO

The mammalian IO is a bilateral structure consisting of rostro-caudally elongated regions of gray matter that are folded and stacked dorso-ventrally and partly separated by thin sheaths of white matter. The complex is customarily subdivided into the principal olive (PO), the medial accessory olive (MAO), and the dorsal accessory olive (DAO). In the following description the detailed parcellations of the rat IO provided by Gwyn et al. (1977), McGrane et al. (1977), and Azizi and Woodward (1987) are used for reference, although we have found it necessary to introduce some modifications, based on our own observations.

In rat, the PO consists of a cell group which, in its central region, separates into two lamellae, a dorsal lamella and a ventral lamella, that are joined ventrolaterally. Azizi and Woodward (1987) describe the MAO as consisting of three lamellae: the caudally located horizontal lamella, the rostral lamella, and the vertical lamella. The horizontal lamella of the MAO consists of subnuclei a and b, situated from lateral to medial, respectively. The b subnucleus forms the caudal pole of the IO. The rostral lamella of the MAO is composed of a single boomerang-shaped nucleus that is described by Azizi and Woodward as the rostral extension of subnuclei b and c. The vertical lamella of the MAO consists of the following subnuclei: the dorso-medially located beta nucleus; the dorsal cap, which is positioned dorsal to the caudal three-fourths of beta; the ventrolateral outgrowth, a rostro-medial extension of the dorsal cap; and the dorsomedial cell column. The vertical lamella also includes part of the subnucleus c, considered by most investigators to be situated ventral to the beta nucleus. Gwyn et al. (1977) note that the dorsomedial cell column fuses with the ventral lamella of the PO caudally and with the tip of the DAO rostrally, where it constitutes with the latter the rostral pole of the IO. The prominent rat DAO consists of a caudally extending dorsal region and a rostrally located ventral region, which are joined laterally at about the mid-olivary level. These regions are referred to as the "dorsal fold" and the "ventral fold" by McGrane et al. (1977), and these terms are adopted in our description.

In our analysis of Nissl stained and immunostained material, we present evidence that the above parcellation of the rat IO may need some modifications with respect to the dorsomedial cell column, the subnucleus c of the MAO, and the subnuclei which form the rostral pole of the IO. We observe that the dorsomedial cell column is restricted to the central region of the IO, between about 1200 μm and 1600 μm from the caudal pole of the IO (Fig. 3, 1344 μm and 1440 μm; Fig. 5b, c). We also observe in serial sections that the rat dorsomedial cell column fuses caudally with the ventral lamella of the PO, whereas rostrally it does not fuse with any other subnucleus of the IO. It terminates far less rostrally than previously established (Gwyn et al. 1977), and therefore does not extend to the rostral pole of the IO. By this restriction, the rostral extent of the IO becomes the exclusive domain of the PO and the DAO, the latter constituting the rostral pole proper (Fig. 5c, d). These boundaries of the dorsomedial cell column agree with descriptions provided by McGrane et al. (1977) and Bernard (1987). Gwyn describes the rostral part of the dorsomedial cell column as fused with the ventral lamella of the PO. McGrane and coworkers and Bernard distinguish this region from the dorsomedial cell column by calling it the dorsomedial cell group. It is located lateral to the dorsomedial cell column, and is considered by Bernard to be a part of the ventral lamella of the PO. Likewise, we include this region with the ventral lamella of the PO. The rostral part of the c subnucleus of the MAO is described by Gwyn et al. (1977) and Azizi and Woodward (1987) as occupying a location ventral to beta, but caudally extending further than beta. Azizi and Woodward (1987) present evidence that the rostral part of the c subnucleus has the same affer-

ent and efferent connections as the beta nucleus. We distinguish the areas described by Gwyn and coworkers and Azizi and Woodward as the caudal extension of c from the rostral part of c. The caudally located subnucleus is not only cytoarchitecturally continuous with beta, but also has the same GAD immunostaining pattern as beta. Therefore, we consider this region as a caudal extension of the beta nucleus (Figs. 1, 4). Bernard (1987) also describes the beta nucleus as extending more caudally than described by Gwyn. The region recognized by Azizi and Woodward as the rostral part of c is considered here as the entire subnucleus c of the MAO (Fig. 4).

Immunocytochemistry

The entire rat IO contains GAD immunoreactive puncta, interpreted as axonal boutons, that occur as isolated or clustered entities and as varicosities of small diameter fiber branches. Most of these puncta are located in the neuropil, but some appear to be closely apposed to olivary cell bodies, and in some cases, outline these GAD-negative somata (Fig. 10). The GAD-positive innervation is dense, although somewhat variable, in all olivary subnuclei. The subnuclei of the IO stand out clearly from the neighboring reticular formation, which contains a lower density of immunoreactive puncta. However, the neuropil of the entire raphe pallidus, located medial and ventral to the IO, is also densely innervated, but is clearly distinguishable from the olive because of its position and relation to the pyramidal tract. The immunocytochemical protocol employed in this study exclusively stains GABAergic boutons, and therefore, no GAD-positive somata were apparent in the IO. A subsequent paper, based on different protocols specifically designed for cell body staining, will describe the occurrence of a small number of GABAergic neurons in the mammalian IO.

Coronal sections. In order to provide a subjectively determined quantitative description of GAD immunostaining throughout the IO, values ranging from 1 to 5 were assigned to individual olivary regions, according to the visually perceived staining intensities of the regions. Intensity scoring was performed directly from microscopic observation, and it must be noted that variations in staining intensity are substantially degraded in low magnification photographs. The following description refers to the coronally cut sections illustrated in Figs. 1–3, which are denoted by their distance, in micrometers, from the caudal pole of the IO. The length of the IO varies in rats of different sizes, and therefore these distances apply specifically to the illustrations obtained from a 180 g rat.

The subnucleus which forms the caudal tip of the IO, labelled subnucleus b of the MAO, stains with an intensity of 2 (Fig. 1, 100 μm). Rostrally, the b subnucleus is joined laterally to the subnucleus a of the MAO at 250 μm (Fig. 1, 280 μm). Medial to the b subnucleus, the caudal tip of beta forms at about 300 μm (Fig. 1, 280 μm and 380 μm). At a more rostral level (Fig. 2, 560 μm), four discrete areas of different staining intensities are present. Proceeding from lateral to medial, an area corresponding to subnucleus a of the MAO is stained with intensity 3 and is contiguous to an area rated 1, corresponding to subnucleus b of the MAO. This area extends toward the midline in a narrow band which may be part of subnucleus c of the MAO. Above this area is a dense region, rated 5, that contains predominantly large and heavily stained puncta, and is interpreted as the beta nucleus. Dorsal to the beta nucleus is the fourth area, rated 4, which clearly corresponds to the dorsal cap (Fig. 4, a and d). At level 1052 μm, the rostrolateral extension of the dorsal cap, the ventrolateral outgrowth, is rated 3. It is contiguous with the rostral part of beta, but is distinguished from it by a lower staining intensity and smaller sized puncta. The beta nucleus maintains the same immunostaining features as in its caudal part. The MAO can be separated here into a medial region, interpreted as the c subnucleus, that is ventral to beta and stains with intensity 4, and a lateral region rated 3 (Fig. 4). This lateral region is part of the rostral lamella of the MAO, as evident in the horizontal plane in Fig. 5c, d. Staining within the PO is also rated 3. The two folds of the DAO are also present at this level. The dorsal fold stains with intensity 1 at its middle, but is rated 3 to 4 at its medial and lateral ends. The ventral fold of the DAO, which laterally joins the dorsal fold, stains with an intensity of 2. At level 1152 μm few changes are observed. The ventral fold of the DAO stains with an intensity of 3, except at its medial end where it joins with the PO and is rated 5. This dense area of staining is also observed at more rostral levels of the IO (Fig. 3, levels 1344 μm and 1440 μm) where it becomes more extensive. The boutons in this region of the ventral fold of the DAO are very densely packed, and this contributes to the intense staining. The rostral edge of the dorsal fold is barely discernible at this level. The rostral lamella of the MAO, the ventrolateral outgrowth and the PO retain the same staining characteristics. Beta separates from the rest of the MAO, and becomes more sparsely innervated, but it contains densely stained boutons of the same size as at caudal levels. The spatial relations described above for the medially located subnuclei in Fig. 2 are shown at higher magnification in the GAD immunostained (a, b, and c) and corresponding Nissl stained (d, e, and f) sections of Fig. 4. Between level 1152 μm and 1344 μm is the transitional zone of Azizi and Woodward (1987), that will be described below in horizontal sections (see Fig. 5a, arrow). At level 1344 μm, the most medial area is interpreted as the dorsomedial cell column, which extends medially from the ventral lamella of the PO. The dorsomedial cell column contains large GAD-immunoreactive puncta that produce a staining intensity of 3. This immunostaining is considerably different from that of the beta nucleus, rated 5, that ends caudal to this level. The rostral lamella of the MAO is rated 3, as in level 1152 μm. The PO is divided into its two lamellae. The dorsal lamella and the medial portion of the ventral lamella are rated 3. The remaining part of the ventral lamella appears sparsely innervated (intensity 1) due to traversing bundles of immunonegative axons. The dorsal fold of the DAO stains with intensity 3, except in the previously described medial region, rated 5, that joins the PO. At 1440 μm, the dorsomedial cell column is distinctly separate from other subnuclei of the IO. The other regions retain the previously described characteristics, with the exception of the ventral lamella of the PO, which is fully represented and stains with intensity 2, as does the dorsal lamella. At level 2018 μm, the dorsomedial cell column is no longer present. No changes are observed in the staining intensities of the rostral lamella of the MAO, the PO, and dorsal fold of the DAO. The rostral pole of the IO is not illustrated in the coronal plane, because it is best evident in horizontal sections.

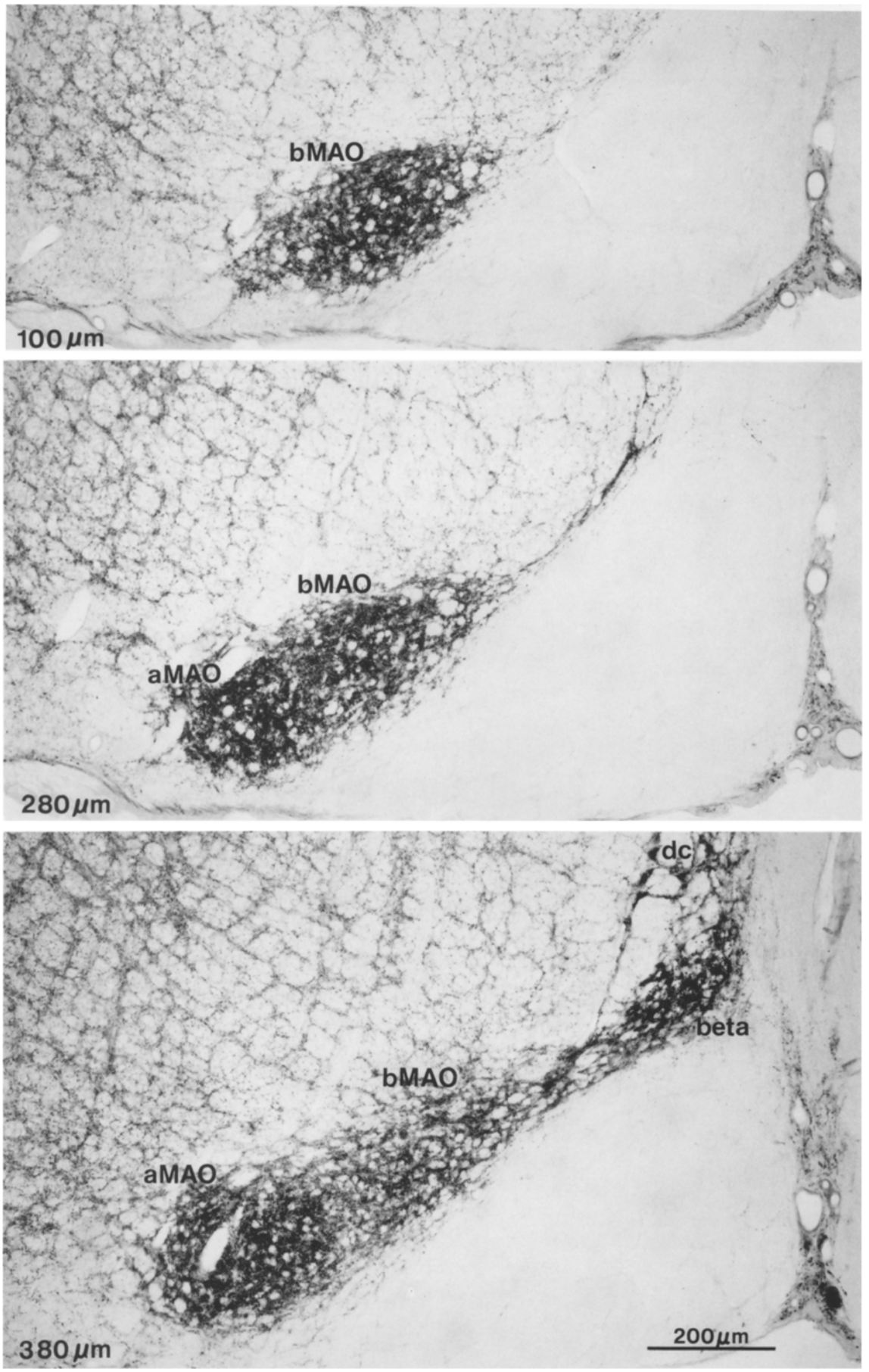

Fig. 1. GAD immunostaining in caudal regions of the rat IO in coronal sections. Distance from the caudal pole of the IO is indicated in the lower-left corner of each photomicrograph. The caudal poles of the beta nucleus and the subnucleus a of the MAO form near level 280 µm

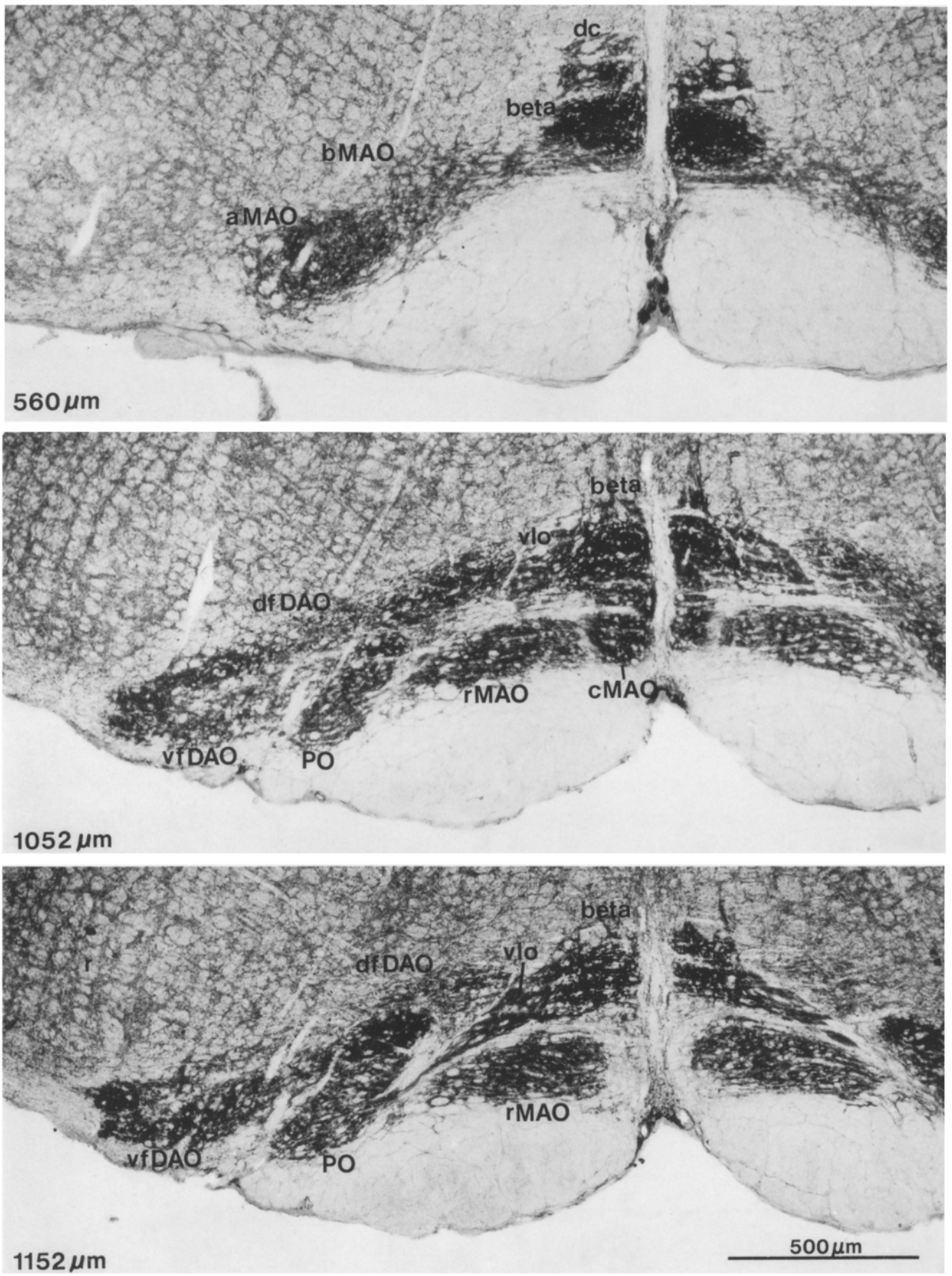

Fig. 2. (For legend see p. 115)

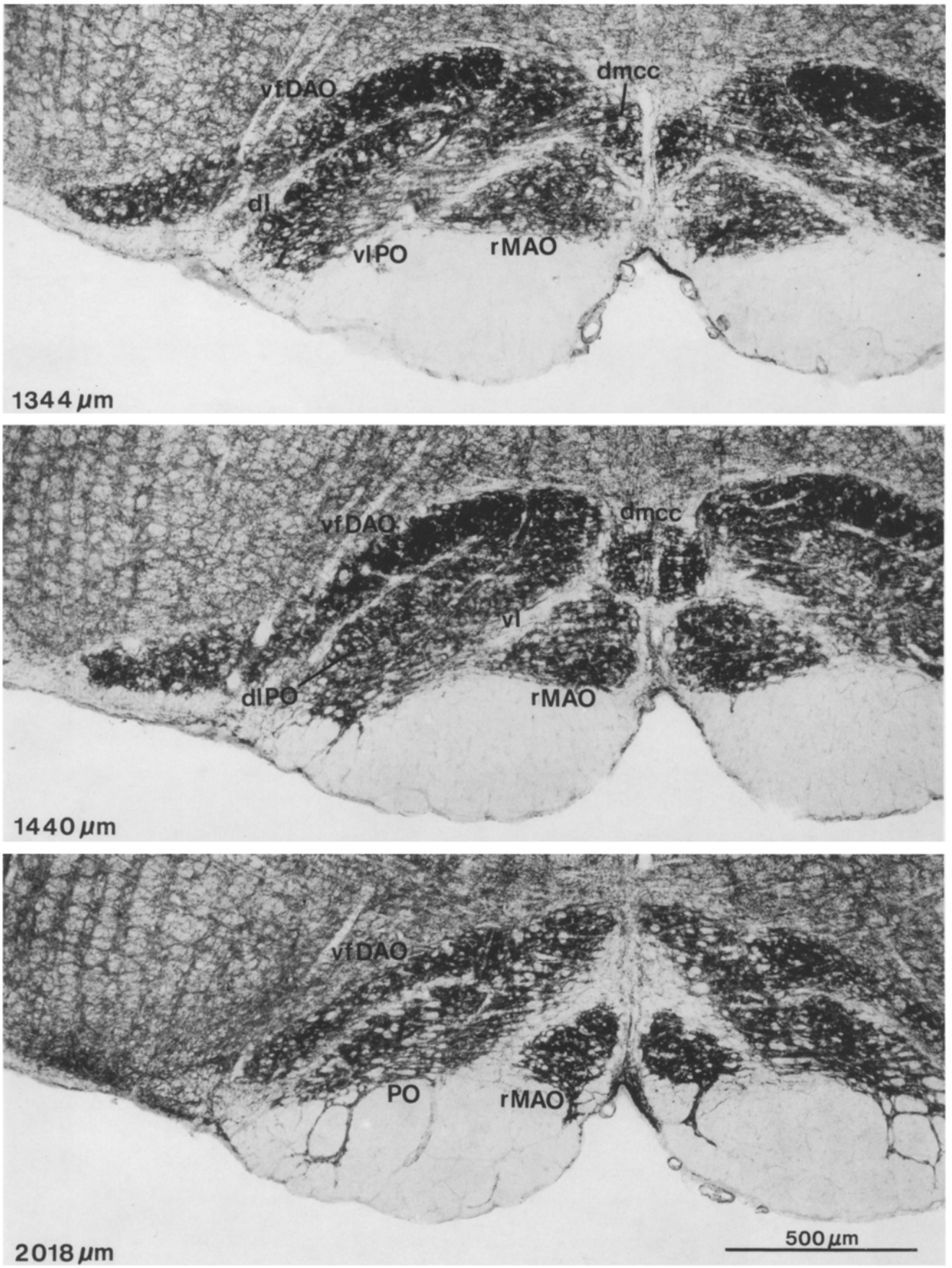

Figs. 2, 3. GAD immunostaining of the rat IO in coronal sections. The entire rat IO is heavily innervated by GAD-positive boutons but regional variations in staining intensity are apparent. The surrounding reticular formation contains a lower density of GABAergic boutons, and the pyramidal tract is GAD-negative. Distance in microns from the caudal pole of the IO is shown in the lower left corner of each photomicrograph

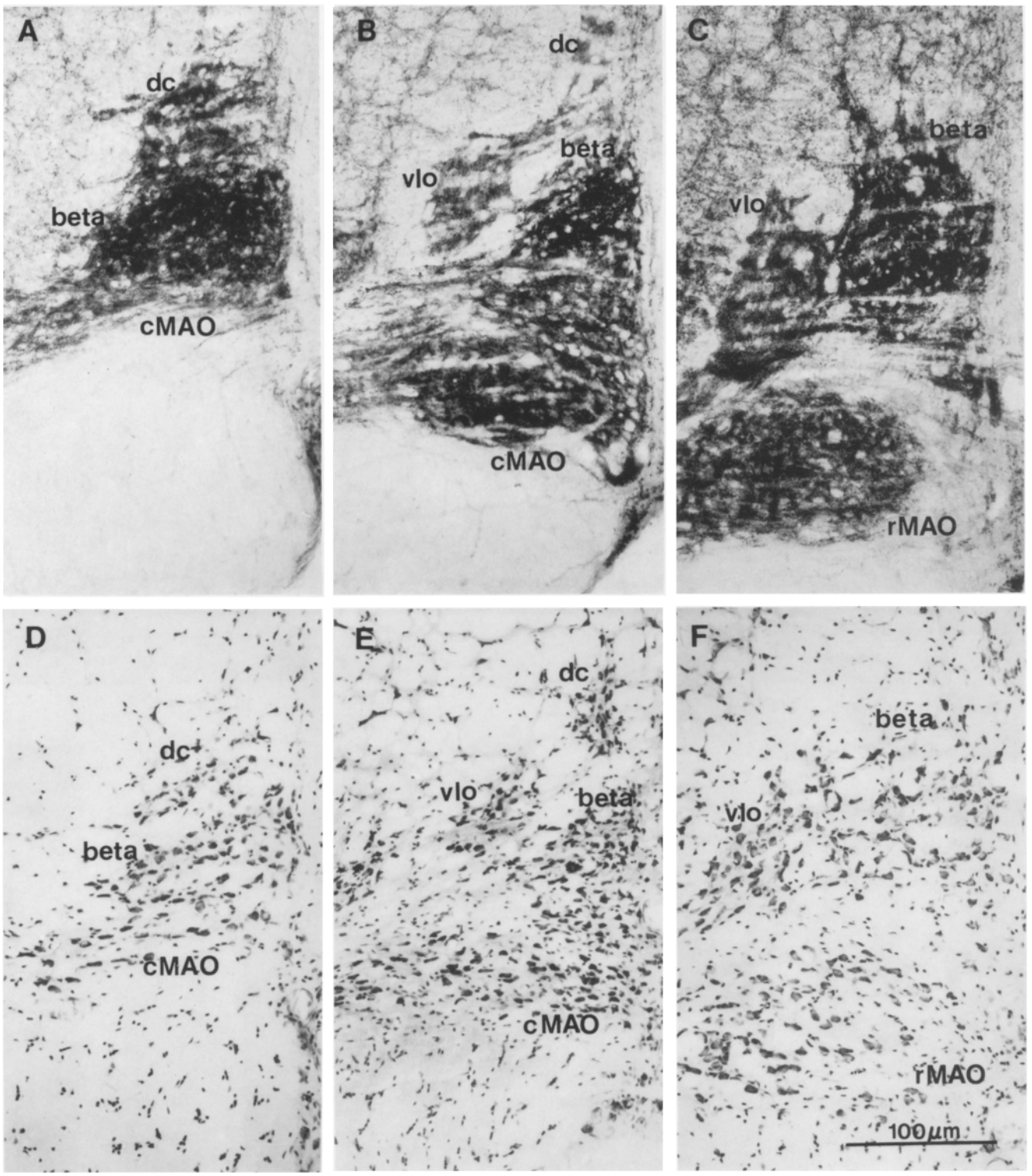

Fig. 4 A–F. Rostral aspects of the beta nucleus, and its relation to the subnucleus c of the MAO and the ventrolateral outgrowth in coronal sections. **A–C** GAD immunostaining clearly defines the boundaries of the medial subnuclei. **D–F** Nissl stained sections at levels corresponding to the sections in **A–C** illustrate the subdivision of this region suggested by GAD immunocytochemistry

Horizontal sections. Sections cut in the horizontal plane clearly show the rostro-caudal extent of the subnuclei, and help to indicate where some subnuclei can be further subdivided by discontinuities in GAD immunostaining patterns. In Fig. 5, four horizontal sections are depicted in dorsal (a) to ventral (d) order with the caudal aspect towards the reader. The IO on both sides of the brainstem midline is illustrated, but the symmetry is imperfect due to a slight tilt in the horizontal plane. The most dorsal section clearly shows the transitional zone of Azizi and Woodward (1987) (Fig. 5a, arrow). This zone separates the DAO into the caudally located dorsal fold and the rostrally located ven-

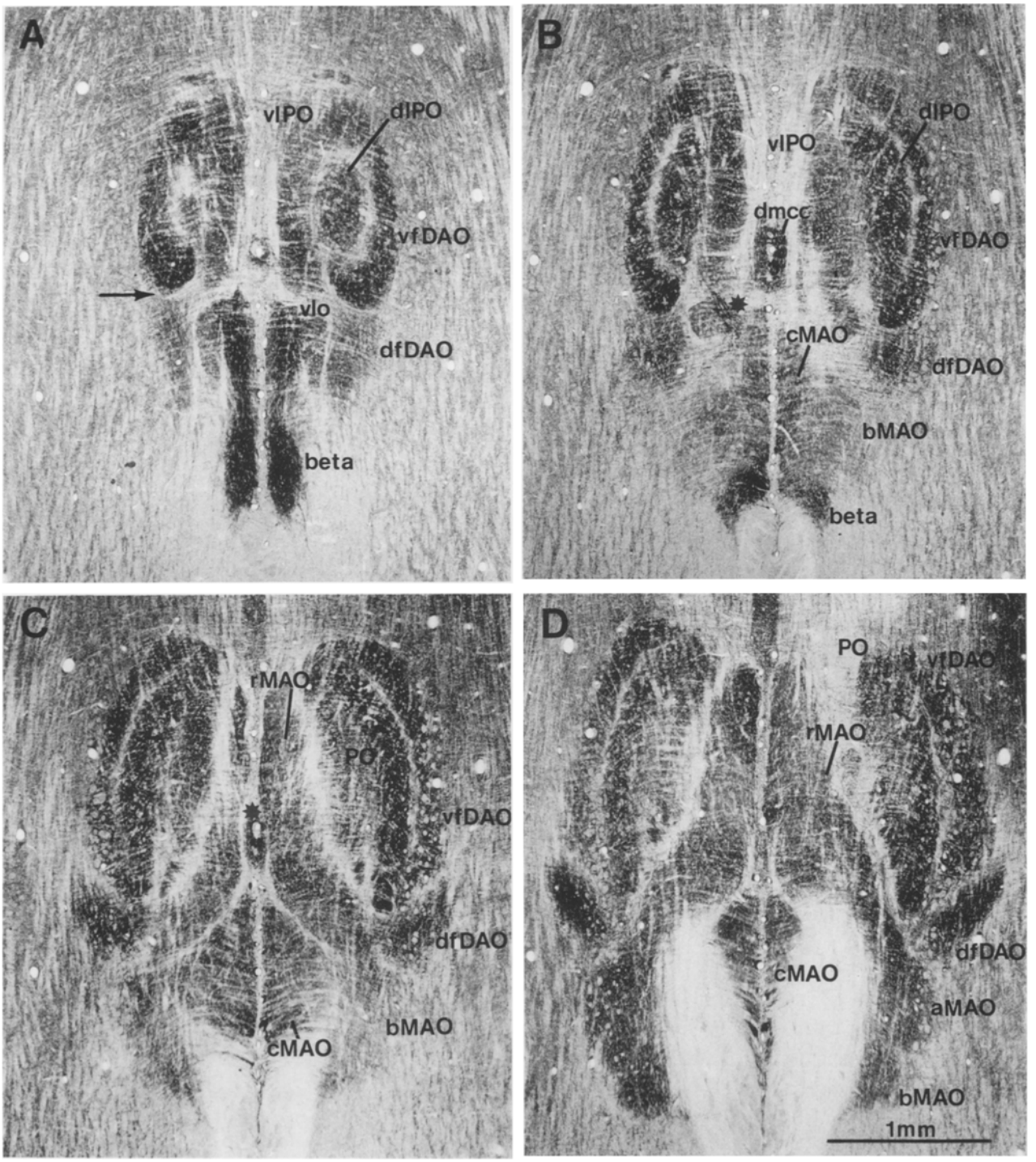

Fig. 5A–D. GAD immunostained horizontal sections through rat IO. Four levels, labelled **A–D**, are arranged in dorsal to ventral order. The caudal aspect of the IO points towards the bottom of the page. *Arrow* in **A** indicates the transitional zone of Azizi and Woodward (1987). *Asterisk* shows ventrolateral outgrowth in **B**, and dorsomedial cell column in **C**

tral fold. The intensity of GAD immunostaining clearly differs in these two parts of the DAO. The dorsal fold is sectioned through its medial region, and is stained less intensely for GAD than all parts of the ventral fold. The caudal end of the ventral fold contains the densely stained region that is visible medially in the coronal plane (Figs. 2, 3, levels 1152 μm to 1440 μm), whereas the remainder of the ventral fold is stained with the same intensity as the PO. In this plane, the PO is present rostral to the transitional zone. The ventral lamella is the most medially located region, and is joined with the dorsal fold of the DAO at the rostral end of this section. The dorsal lamella is surrounded medially by the ventral lamella and laterally by the ventral fold of the DAO. At the transitional zone, the beta nucleus and the centrally located dorsomedial cell column appear markedly separated by white matter. The entire

rostro-caudal extent of beta is evident by virtue of its extremely intense immunostaining. Contiguous with beta laterally is the less intensely stained ventrolateral outgrowth. At a more ventral level (Fig. 5b), only the caudal tip of beta is present. The rostral tip of beta (asterisk) is also seen on the left side of the brainstem with the ventrolateral outgrowth located lateral to it. A large area ventral to beta is more intensely stained medially than laterally. The lateral, weakly stained area is interpreted as the b subnucleus of the MAO, and the more intensely stained medial region as the c subnucleus. The dorsal fold of the DAO is stained more intensely than in dorsal sections, as the lateral part of this subnucleus is now visible. The PO is separated into the medially located ventral lamella, and the more laterally located dorsal lamella. On the right side of the brainstem, the junction of the dorsal lamella of the PO and the ventral fold of the DAO is visible, and is intensely stained for GAD. The main body of the dorsomedial cell column is bisected by the brainstem midline. In Fig. 5c, the subnucleus c of the MAO is clearly continuous with the relatively pale b subnucleus, but is separated from the rostral lamella of the MAO. On the right side of the brainstem, the b subnucleus fuses with the rostral lamella of the MAO. The ventral tip of the dorsomedial cell column (asterisk) is visible at the midline, between the two sides of the rostral lamella of MAO, and maintains the same staining intensity as at dorsal levels. At this ventral level, the densely stained medial region of the DAO ventral fold is not present in the section, because the DAO and the PO extend ventrolaterally. No substantial changes occur in the staining of these subnuclei. In Fig. 5d, the caudal pole of the IO is visible and is formed by a relatively densely stained region of subnucleus b. About 250 μm rostral to the caudal tip of the IO, the subnucleus a forms lateral to the subnucleus b, and is continuous rostrally with the rostral lamella of the MAO. (See also Fig. 1.) The lateral region of the DAO dorsal fold remains separate from the less intensely stained ventral fold. On the right side of the brainstem, the ventral and dorsal lamellae of PO are fused, as the section contains the lateral region of the PO.

Sagittal sections. Two immunostained and one Nissl stained sagittal series were evaluated in order to further clarify the boundaries of some subnuclei. Sections from one of these sagittal series, illustrated in Fig. 6, are used to complement the descriptions presented above. To avoid redundancy, we do not provide a detailed description of all of the subnuclei depicted in the sagittal plane.

The sections that comprise Fig. 6 are ordered from medial to lateral, with the distance from the brainstem midline indicated in each photograph. At level 110 μm, the densely stained beta nucleus is present throughout its rostrocaudal extent. The more sparsely stained dorsal cap is situated above the caudal two-thirds of beta. The subnucleus c of the MAO is situated ventral to most of the caudorostral extent of beta, and is less intensely stained for GAD in its caudal aspect than it is rostrally. In this sagittal view of subnucleus c, it is apparent that the area contiguous with the ventral boundary of beta, depicted in Fig. 2, level 560 μm, is part of the subnucleus c of the MAO. In level 190 μm, the subnucleus c comprises most of the caudal MAO, although the lateral edges of beta are present at mid-olivary level. The rostral half of the section contains the ventral lamella of the PO and the rostral lamella of the MAO, but is lateral to the dorsomedial cell column. Level 420 μm contains the b subnucleus of the caudal MAO. No clear separation between the subnucleus b and the rostral MAO is apparent. The densely stained area of the ventral fold of the DAO is fused caudally with the dorsal lamella of the PO. Section 660 μm contains both subnuclei a and b of the MAO, the subnucleus a being located caudal to the lighter staining subnucleus b. Level 710 μm is entirely lateral to subnucleus b, as indicated by the closeness of the caudal aspect of the IO to the ventral surface of the brainstem. The subnucleus that extends most rostrally at levels 420 μm, 660 μm, and 710 μm is the ventral fold of the DAO. The IO extends furthest rostrally in levels 660 μm and 710 μm, and, therefore, the ventral fold of DAO forms the rostral pole of the IO.

General remarks. For the most part, regional differences in GAD immunostaining intensity follow the subnuclei boundaries of the IO. A notable exception is the ventral fold of the DAO, which contains a region of more intense staining where it joins the PO medially and the dorsal fold of the DAO laterally. Other apparent changes in staining intensity within a given subnucleus, such as in the ventral lamella of the PO, the dorsal fold of the DAO, and the rostral region of subnucleus b of the MAO can be attributed to predominant immunonegative fibers passing through these regions. Furthermore, it appears that certain subnuclei share the same staining intensity, most notably the PO, the rostral lamella of the MAO, and the lateral part of the DAO ventral fold.

Photometric analysis

In order to substantiate the large scale differences in GAD immunostaining that are visually apparent among the various subdivisions of the IO, a relatively more objective measure of focal immunostaining intensities was obtained photometrically with a spot light meter (see also Discussion). Regions with predominant GAD-negative fiber bundles were avoided during the photometric analysis (see Methods). Intensities of regions vary among rats (Table 1). Average regional values, expressed as a percent of the most intensely stained region, the beta nucleus, are shown in Fig. 7. Values obtained from the medial part of the ventral lamella of the DAO (91.9%), were close to those from the beta nucleus. The c subnucleus of the MAO measured 67.6%. The dorsal cap, the dorsal fold of the DAO and the dorsomedial cell column average from 47.2% to 57.6%. The lateral part of the ventral fold of the DAO, the rostral MAO, the PO, and the ventrolateral outgrowth have the lowest intensities, ranging from 26.0% to 42.8%. Subnuclei a and b of the MAO also stain with low intensities, but all parts of the subnucleus b have slightly lower values than the subnucleus a. Examples of these regions are depicted in Fig. 8. Although a large variation in values occurs within regions (see standard deviations in Table 1), these values reflect fairly well the visually apparent differences of staining in these areas. An exception is the dorsomedial cell column, which receives a lower intensity rating in the visual analysis scale than in the photometric analysis scale. This discrepancy may be due to the greater spatial resolution of the photometric method, which measures staining intensity only within the neuropil, than the visual analysis, in which staining intensity was assigned to an entire region.

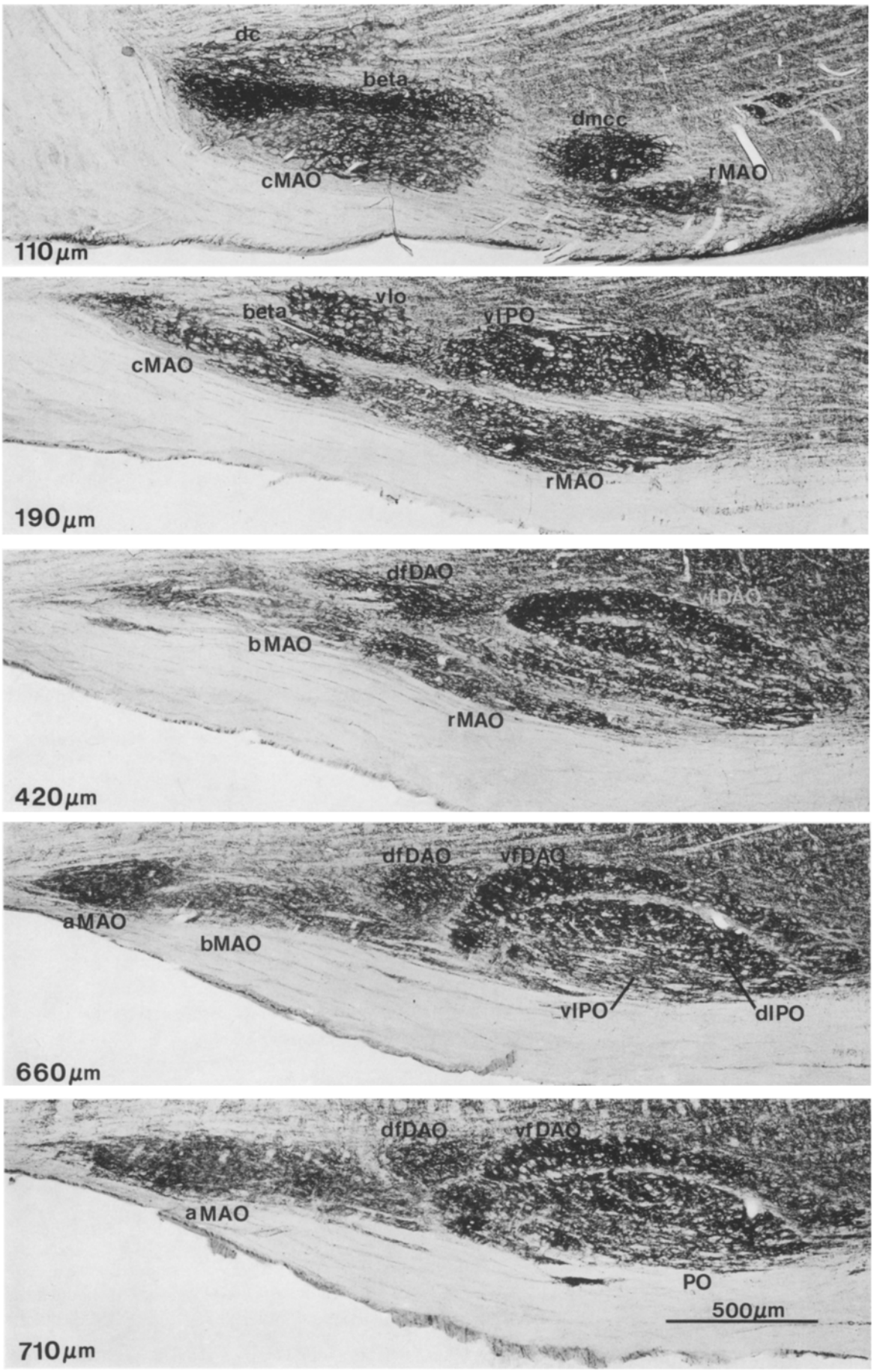

Fig. 6. GAD immunostained sagittal sections through rat IO. The rostro-caudal extent of many olivary subnuclei can be observed in this plane. Approximate distance from the brainstem midline is indicated in the lower left corner of each photomicrograph

Table 1. GAD immunostaining intensity[a] in the rat IO

Region	Rat 3799	Rat 3800	Rat 3801
Beta	12.02±0.78	9.92±1.04	11.54±1.51
Medial ventral fold DAO	9.94±0.84	9.80±1.26	10.88±0.96
cMAO	9.08±0.86	6.94±0.46	6.60±1.18
Dorsomedial cell column	6.25±0.33	6.83±0.46	5.98±0.15
Dorsal fold DAO	6.36±0.67	5.16±0.85	4.22±0.57
Dorsal cap	6.34±1.12		5.08±0.60
aMAO	5.64±0.49	3.58±0.84	4.66±0.45
bMAO	4.22±0.69	3.36±0.42	3.48±0.51
Ventrolateral outgrowth	4.80±0.54	3.60±0.21	4.06±0.13
Rostral lamella MAO	5.24±0.56	4.02±0.50	3.46±0.42
PO	4.82±0.58	4.75±0.30	3.40±0.20
Lateral ventral fold DAO		3.23±1.28	4.73±0.93

[a] Mean intensities±SD ($n=5$ for all cases) are presented for three different rats to indicate range of variability among specimens. Staining intensity was measured photometrically as exposure time (s) at ASA 12 with a Nikon Microphot spot light meter. These values were obtained by subtracting exposure time measured in the immunonegative pyramidal tract from exposure time measured in a given region of IO

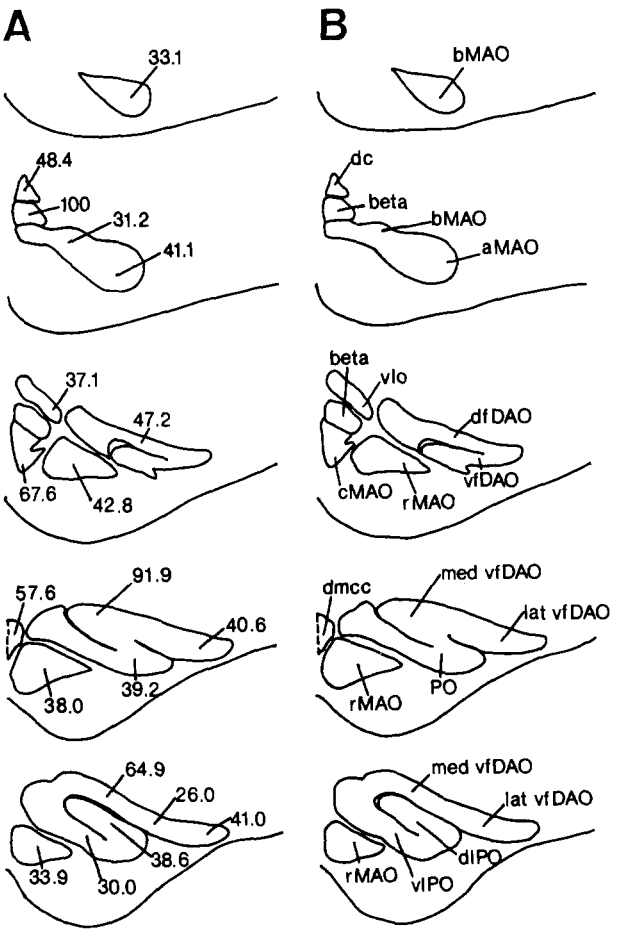

Fig. 7. **A** Diagram summarizing regional immunostaining intensities measured photometrically in rat IO. The individual values given here are the averages from the three rats presented in Table 1, and are expressed as percent of the exposure time measured in the beta nucleus, the most intensely stained region. **B** Diagram showing nomenclature of the IO subdivisions

Due to the limited scope of these measurements and the multifactorial nature of immunocytochemical staining (see below), we did not attempt to statistically compare staining intensities among regions.

Analysis of individual bouton characteristics

Since the photometrically determined staining intensities in a given region depend on the density of boutons in the region and the bouton size, in addition to individual bouton staining intensity, an analysis of individual bouton characteristics was performed in an attempt to further clarify the regional differences in GAD immunostaining. The product of long and short diameters ('areas') of individual immunoreactive puncta and the density of puncta were measured from photomicrographs of eleven different olivary regions (Table 2). Staining intensity of individual puncta was not determined. The sections used for this analysis were cut 2 μm thick from plastic embedded tissue in order to obtain optimal resolution of particle edges. With the GAD antiserum and the protocol used in this study, GABAergic myelinated axons in the IO stain only weakly (see also Gotow and Sotelo 1987), although such axons are densely stained by antisera against GABA itself (Ottersen and Storm-Mathisen 1984). Furthermore, immunoelectron microscopy (our unpublished observations; Sotelo et al. 1986) indicates that preterminal axons, which have diameters of less than 0.5 μm, are substantially smaller than the GABAergic boutons in the IO (see arrowheads in Fig. 10). Bouton diameters ranged from 0.85 μm to 3.9 μm, and we therefore presume that the vast majority of the puncta measured in this study were axonal boutons. It is possible that some GAD-positive particles measured as one bouton were actually two contiguous boutons, thus resulting in an overestimate of bouton sizes, particularly in densely innervated regions. However, we tried to reduce this error by including only particles in one focal plane that lacked visible irregularities along their edges. Thus, in the following account, puncta will be referred to as "boutons". Bouton fragments were certainly included in the study, but no correction for this factor was attempted. It should be noted that within each region, the GABAergic boutons are by no means homogeneous, but rather, they range considerably not only in size, but also shape (Fig. 10).

Table 2 lists the mean areas of boutons populating eleven olivary regions. GAD-positive boutons in the beta nucleus have the largest mean area, and those in the rostral lamella of the MAO have the smallest mean area. An analysis of bouton area variance in the eleven olivary regions reveals highly significant differences by region ($F=22.48$, 10/319 df; $p<0.0001$). Multiple comparisons of mean areas among the eleven regions delineated four groups (denoted A to D in Fig. 9), which partly overlap. Group A is formed by boutons in the beta nucleus only, which average 5.04±1.71 μm^2. Group B contains the boutons in the dorsomedial cell column, dorsal cap and the dorsal fold of the DAO. Mean bouton areas of these regions range from 3.33±0.85 μm^2 to 3.72±1.01 μm^2. The boutons of the dorsal cap and the dorsal fold of the DAO do not differ significantly from those in the medial part of the ventral fold of the DAO, and these three regions form group C. Mean bouton areas of group C range from 2.92±0.79 μm^2 to 3.39±0.86 μm^2. Group D contains boutons located in the a, b and c subnuclei of the MAO, the lateral part of the

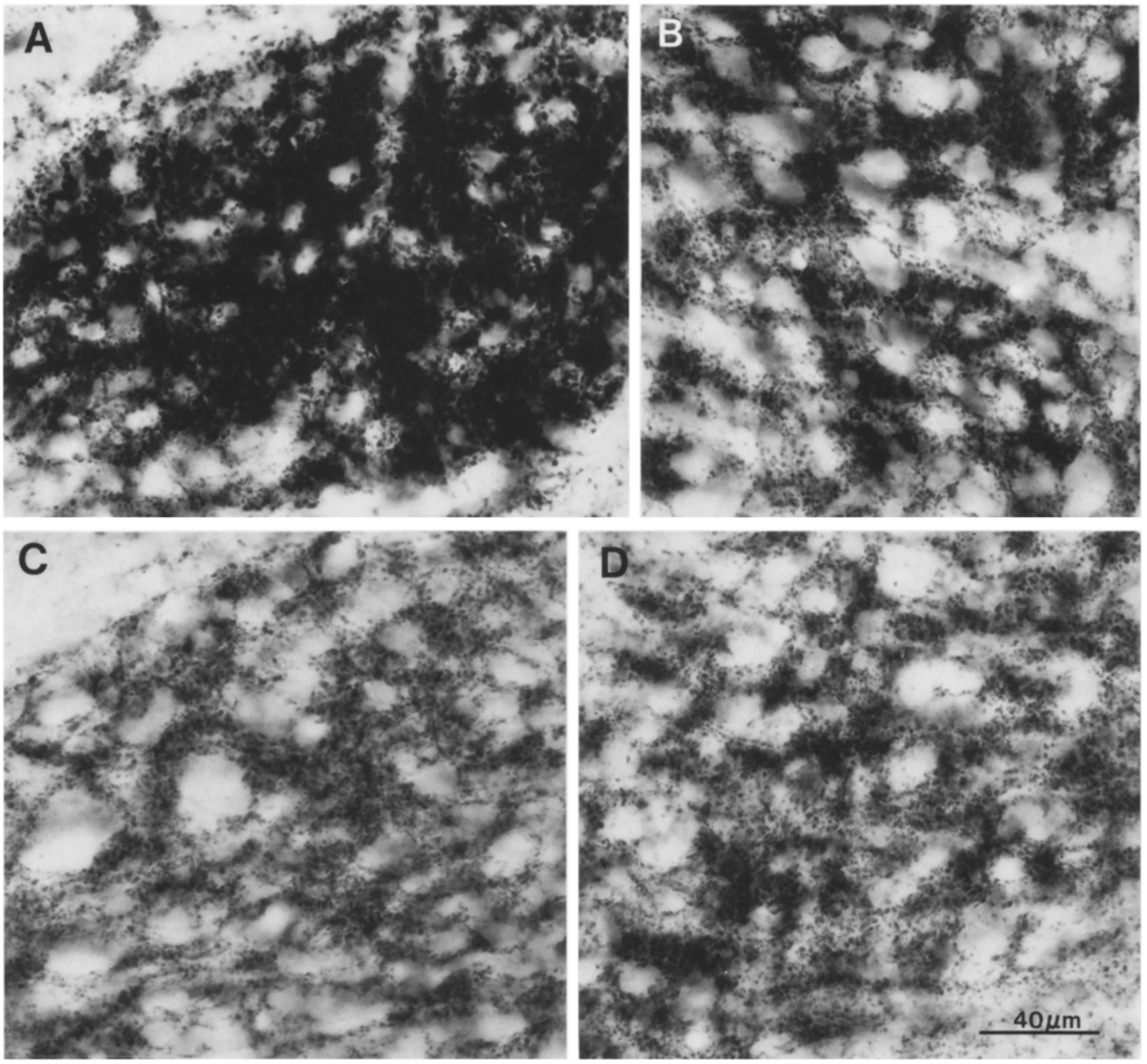

Fig. 8A–D. GABAergic boutons in four representative regions of the IO which have different photometrically determined staining intensities. **A** Beta nucleus. **B** Subnucleus c of MAO. **C** Rostral lamella of MAO. **D** Dorsal fold of DAO

ventral fold of the DAO, the PO, and the rostral lamella of the MAO, which range in area between $2.39 \pm 0.86\ \mu m^2$ and $2.61 \pm 1.04\ \mu m^2$. These boutons differ significantly from all members of groups A and B ($p < 0.05$). The boutons in the medial part of the ventral fold of the DAO do not differ significantly from those of any region of group D, or from those of the dorsal cap or the dorsal fold of the DAO. Therefore, boutons in the medial ventral fold of the DAO are included in group D as well as group C. GAD immunostaining in semithin sections from regions representing each of these four groups is illustrated in Fig. 10.

The densities of GAD-positive boutons in eleven different regions of the IO are also presented in Table 2. Only the medial part of the ventral fold of the DAO has an outstanding density of GABAergic boutons as compared to other regions, which probably accounts for the high intensity ratings obtained from the photometric and visual analyses (Fig. 10c).

Discussion

The rat inferior olive contains a great abundance of GAD immunoreactive puncta, generally considered to be GABAergic presynaptic axonal endings. Since GABA is known to produce inhibitory responses at CNS synapses (reviewed by Krnjević 1976), it is a good candidate for a neurotransmitter which produces olivary inhibition. GABAergic boutons are mostly present in the olivary neuropil, indicating that they presumably synapse on dendrites and possibly

Table 2. GAD-positive bouton area and density in regions of rat IO

Region	Mean bouton area[a] (μm^2)	Mean density[b]
Beta	5.04±1.71	28
Dorsomedial cell column	3.72±1.01	19
Dorsal cap	3.39±0.86	23
Dorsal fold DAO	3.33±0.85	17
Medial ventral fold DAO	2.92±0.79	47
cMAO	2.61±1.00	29
bMAO	2.55±0.71	20
aMAO	2.48±0.65	22
PO	2.46±0.54	26
Rostral lamella MAO	2.38±0.71	26
Lateral ventral fold DAO	2.48±0.91	23

[a] Bouton area is the product of long and short bouton diameters. Bouton areas in each region were averaged to obtain mean bouton area ±SD. $N=30$ boutons per region

[b] Density is the number of immunoreactive boutons per area of 400 μm^2. $N=6$ areas per region

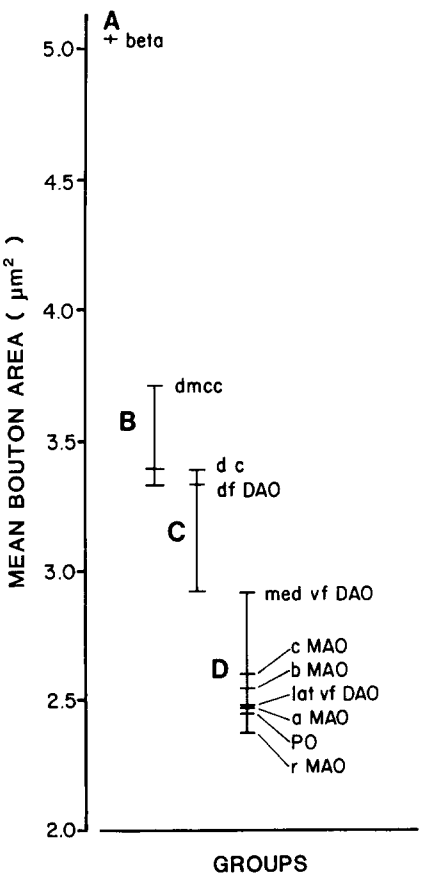

Fig. 9. Grouping of GABAergic boutons by mean bouton area. Letters *A–D* denote four groups of values defined by multiple comparisons of mean areas in eleven regions of the rat IO (Ryan-Einot-Gabriel-Welsch multiple range test). Means within a group are not significantly different ($P>0.05$). Regions that compose group *C* (dorsal cap, dorsal fold of DAO and medial ventral fold of DAO) have means which overlap with those of groups *B* and *D*. Mean areas and standard deviations used to make comparisons are listed in Table 1

are components of glomeruli. These suggestions have been verified at the EM level by ourselves (Mugnaini, unpublished overview lecture, Soc Neuroscience 1985; Nelson and Mugnaini 1985), and by Sotelo et al. (1986). Many GABAergic synapses are situated in close proximity to gap junctions, which may be the morphological basis for the notion that GABA neurotransmission uncouples principal neurons in the IO with a mechanism similar to that present in Navanax buccal ganglion (Llinás et al. 1974; Sasaki and Llinás 1985; Sotelo et al. 1986; Spira and Bennett 1972; Spira et al. 1980). In addition, a substantial number of GABAergic puncta synapse on dendrites and cell bodies, and occasionally are present also on initial axon segments, locations that suggest inhibition of climbing fiber activity occurs via GABA neurotransmission (Andersson and Hesslow 1987a, b; Barmack et al. 1987). The presence of GABAergic synapses on virtually every portion of the receptive surface of olivary neurons and in every part of the IO indicates that GABAergic modulation of climbing fiber activity is a universal feature of the olivary circuitry.

GAD immunostaining intensity varies within the IO. To shed light on the significance of this heterogeneity, we graded GAD immunostaining intensity visually and photometrically. Visual examination was useful in establishing a chemoarchitectural map of the IO, while the photometric analysis provided focal measurements of staining intensities within the neuropil areas of different subnuclei. In addition, we measured the size and density of immunostained puncta in various regions. Our photometrically determined measures of immunostaining and analysis of individual GABAergic bouton characteristics are consistent with visually determined regional differences in the GABAergic innervation. In general, these regional variations are consistent with the compartments drawn for the mammalian IO based on climbing fiber projections to the cerebellar cortex. The variation in GAD immunostaining may be due, at least in part, to the existence of different GABAergic afferent pathways to subregions of the IO.

Parcellation of GAD immunostaining in rat IO

Functional subdivisions of the mammalian IO, especially in cat and monkey, have been delineated mainly on the basis of the distribution of olivary afferents and climbing fiber projections. The organization of the climbing fiber projections in rat is essentially similar to that of cat and monkey (review of Brodal and Kawamura 1980; Campbell and Armstrong 1983b; Wiklund et al. 1984). However, the precise subdivision boundaries of the rat IO have been debated. Since climbing fiber projections to the cerebellar cortex are topographically arranged, a correct evaluation of IO subdivisions is crucial to obtain an understanding of olivary function, and for drawing comparisons of its organization and function between species. The regional differences in GAD immunostaining offer a particular view of the organization of the IO. Overall, we find that subdivisions of the rat IO evident in GAD immunostained sections largely coincide with divisions of the IO determined by the zonal organization of climbing fibers in the cerebellar cortex that have been developed largely for cat and monkey cerebella.

The rat DAO is subdivided by McGrane et al. (1977) and Azizi and Woodward (1987) into a rostrally located ventral fold and a caudally located dorsal fold, based on

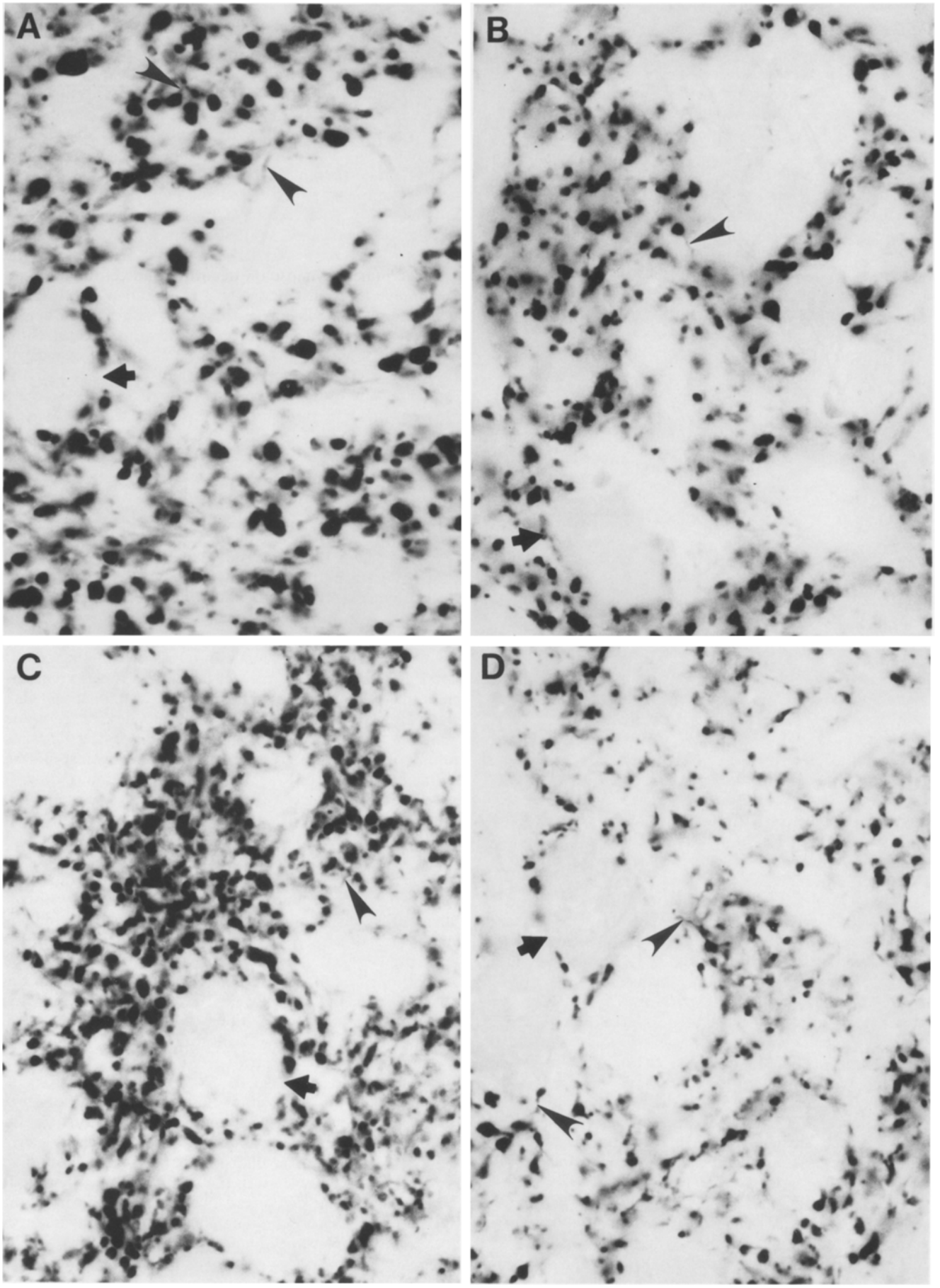

Fig. 10A–D. These photographs of plastic embedded sections used to measure bouton areas and density show GAD-positive boutons in four regions of rat IO. **A** Beta nucleus. **B** Dorsal fold of DAO. **C** Medial region in the ventral fold of DAO. **D** Rostral lamella of MAO. *Arrows* in each photograph point to olivary principal (GAD-negative) neurons delineated by GAD-positive boutons. *Arrowheads* indicate small diameter processes, which are probably unmyelinated axons. × 1800

cytoarchitecture and climbing fiber projections. These divisions are clearly seen in coronal sections immunostained with GAD (Fig. 2, levels 1052 μm and 1152 μm). A distinction has also been made between rostral and caudal parts of the cat DAO based on climbing fiber projections to the cerebellar cortex (reviewed by Brodal and Kawamura 1980). The feline caudal DAO projects to zone B of the cerebellar cortex, while the rostral DAO projects to zones C1 and C3. Like the corresponding areas in the feline DAO, the ventral fold of the DAO in rat projects to the intermediate cerebellar cortex, while the dorsal fold projects to the vermal anterior lobe (Azizi and Woodward 1987; Campbell and Armstrong 1983b). A separation of the rat DAO into two subdivisions is supported by GAD immunostaining differences in the ventral and dorsal folds.

The ventral fold of DAO can be further subdivided into a medially located region that is densely GAD immunoreactive, and the remainder of the subnucleus, which stains less intensely. This difference may have some functional significance, since these two regions of the rat DAO project to different areas of the cerebellar cortex: the medial part of the DAO projects to the intermediate cortex of crus I and II, while the climbing fiber projection of lateral DAO is to the intermediate cortex of lobules III and IV (Azizi and Woodward 1987).

The rostral MAO may likewise be considered as a functional unit distinct from the caudal subnuclei of MAO, based on climbing fiber topography and GAD-immunostaining. Azizi and Woodward (1987) describe the rostral lamella of the MAO, which projects to intermediate regions of the cerebellar cortex, as distinct from the caudally located vertical and horizontal lamellae, which send climbing fibers to vermal cerebellar lobules. These projections have also been observed by Brown (1980) and Campbell and Armstrong (1983b). McGrane et al. (1977) also describe a climbing fiber projection from rostral MAO to the cerebellar hemispheres, but they subdivide the caudal MAO into a medial part, which projects to the posterior vermis, and a lateral part which projects to the anterior vermis. As is the case with the DAO, this division of the rat MAO into rostral and caudal areas is similar to a division that has been made in the cat MAO (Brodal 1976; Brodal and Walberg 1977; Hoddevik et al. 1976). In the cat, the caudal MAO projects to zone A in the vermal cerebellar cortex, and the rostral MAO projects to zone C2 in the intermediate cortex, and to the paraflocculus (Groenewegen and Voogd 1977). By GAD immunocytochemistry, the rostral lamella of the MAO can be distinguished from the caudally located c subnucleus. The a and b subnuclei are stained like the rostral lamella of the MAO.

The boundaries of the c subnucleus of MAO must be clarified. In coronal sections (Fig. 2, 1052 μm; Fig. 4) and in horizontal sections (Fig. 5c, d) the c subnucleus of the MAO is situated ventral to beta, and is spatially separate from the laterally located rostral lamella of the MAO. These boundaries are consistent with those described for the rostral part of c by Azizi and Woodward (1987). This region of the rat IO is included in the beta nucleus by Sotelo et al. (1986). This area of the rat IO provides climbing fibers to vermal lobules VI and VII of the cerebellar cortex (Azizi and Woodward 1987; Brown 1980; Furber and Watson 1983; Wiklund et al. 1984) making it homologous to the medial MAO of the cat IO (Hoddevik et al. 1976) and the b subnucleus of the rhesus monkey MAO (Brodal and Brodal 1981). Since climbing fiber projections and GAD immunostaining pattern of this area are different from those of the beta nucleus and the remainder of the MAO, the subnucleus c should be considered as a discrete unit of the MAO. The area described by Gwyn et al. (1977) as subnucleus c contains GABAergic boutons of the same size and the same immunostaining intensity as the beta nucleus, and therefore, we have considered this area as part of beta. We thus propose that beta extends further caudally than previously established.

The rostral extent of beta (Fig. 2, level 1152 μm; Fig. 4) is not clearly specified by Gwyn et al. (1977). Sotelo et al. (1986) label this area the ventrolateral outgrowth, although it has the same GAD immunostaining pattern as the caudal part of beta. However, the ventrolateral outgrowth is labelled less intensely for GAD than beta, and is located lateral to it (Fig. 2, levels 1052 μm and 1152 μm; Fig. 4b, e; Fig. 5a). We agree with Gwyn's group, who describe the ventrolateral outgrowth as a rostro-lateral extension of the dorsal cap, as seen also in cat, rabbit (Brodal 1940), and monkey (subnucleus f of Bowman and Sladek 1973).

The boundaries of the rat dorsomedial cell column are controversial. Gwyn and coworkers claim that the dorsomedial cell column fuses rostrally with the DAO and the PO, but ignore the medially located caudal extension of the nucleus, which they depict in a Nissl stained section (Gwyn et al. 1977, their Fig. 3). The spatial relationship between the dorsomedial cell column and the surrounding subnuclei evident in Fig. 3 (levels 1344 μm to 1440 μm) and Fig. 5b, c is consistent with the cytoarchitecture of homologous areas in cat, rabbit, and rhesus monkey, except that in cat and rabbit, but not in rat or monkey, the dorsomedial cell column fuses rostrally with the MAO (Bowman and Sladek 1973; Brodal 1940; Whitworth and Haines 1986). In GAD immunostained material, the dorsomedial cell column is seen as a medial outgrowth of the ventral lamella of the PO caudally (Fig. 3, level 1344 μm), and becomes an isolated group of cells rostrally (Fig. 3, level 1440 μm; Fig. 5). This cytoarchitectural feature is also evident in Nissl stained material (data not shown). We find that the dorsomedial cell column is only about 400 μm long rostrocaudally. Contrary to the previous notion that it spans the entire rostral half of the IO, we conclude that the dorsomedial cell column does not extend to the rostral pole of the IO. The climbing fiber projections of the dorsomedial cell column in rat are similar to those in cat. In both species, the dorsomedial cell column projects to intermediate zone A2 of the uvula (Groenewegan and Voogd 1977; Groenewegan et al. 1979; Eisenman 1984).

Regional variations in GAD immunostaining

Five regions in the IO are characterized by visually apparent differences in GAD immunostaining intensity. The beta nucleus and medial region of the ventral fold of the DAO are stained for GAD with the highest intensity of 5. The subnucleus c of the MAO forms a second region rated 4. The dorsal cap, the dorsomedial cell column and the dorsal fold of the DAO are similarly labelled and form a third group rated 3. The PO, the lateral part of the ventral fold of the DAO, the ventrolateral outgrowth, and the rostral lamella of the MAO are grouped as one unit based on similarities of GAD immunostaining intensity. Also, the subnuclei a and b of the MAO are included in this latter

group, which has the lowest staining intensity in the IO. These regions are assigned an intensity rating of 2. A rating of 1 is assigned to the rostral part of the subnucleus b of the MAO and to part of the ventral lamella of the PO, regions that are traversed by large bundles of GAD-negative axons.

GAD immunostaining intensities measured photometrically differ substantially in the regions rated 5 through 1 by visual analysis. The greatest photometrically determined values of intensity are observed in the beta nucleus and the medial part of the ventral fold of the DAO, and the lowest values are observed in the PO, the rostral lamella of the MAO, the ventrolateral outgrowth, and the lateral part of the ventral fold of the DAO. Staining intensity varies greatly when comparing subnuclei intensities among individual rats, and therefore are presented as a percentage of maximum staining (observed in the beta nucleus). However, the relative intensity differences of olivary subnuclei within individuals are similar for all three rats, and are consistent with the visually graded intensity levels.

The relationship of GAD immunostaining intensity to regional variation in GABAergic bouton size and density

Several components contribute to the overall GAD immunostaining observed with low power lenses. Two of these components, bouton area and the number of boutons per unit area, were analyzed in several regions of the IO. Possibly a third factor, the concentration of GAD within individual boutons, may contribute to staining intensity, but a precise analysis of this parameter was beyond our technology.

Statistical analysis of mean bouton area reveals the presence of three different sizes of GABAergic boutons in the rat IO. The beta nucleus contains the largest boutons; the dorsal cap, the dorsal fold of the DAO, and the dorsomedial cell column contain intermediate sized boutons; and the a, b and c subnuclei of the caudal MAO, the rostral lamella of the MAO, the PO, and the lateral ventral fold of the DAO contain the smallest boutons. Photometrically measured staining intensities are consistent with this grouping. The medial region of the ventral fold of the DAO is not distinguished by bouton size from the dorsal cap, the dorsal fold of the DAO, or from any of the regions containing small boutons.

By photometric analysis the medial part of the ventral lamella of the DAO is grouped with the beta nucleus. Particle analysis, however, reveals that this intensely stained part of the DAO contains GABAergic boutons with a significantly smaller mean area than the boutons in the beta nucleus. The mean area of these boutons in the DAO does not differ from the populations of intermediate or small GABAergic boutons. GABAergic boutons populate the medial ventral fold of the DAO with an extremely high density as compared to other regions of the IO, a feature which probably accounts for the high staining intensity observed in this region.

Particle analysis draws no distinction between the subnucleus c of the MAO and the group assigned a low intensity rating by photometric analysis, which includes the PO and the rostral lamella of the MAO. The GABAergic bouton area and density in the subnucleus c may be great enough to account for the high immunostaining intensity observed with visual and photometric methods. Immunostaining intensity of individual boutons in the c subnucleus may also contribute to the high field measurement values of intensity, more so than in other regions of the IO.

The purpose of the analysis of GABAergic bouton size was to detect differences by region. A correct analysis of bouton morphometry is best achieved by electron microscopy, although such an approach is easily fraught with limited sample size. The method that we have employed allowed rapid collection of a fairly large sample size from many easily identified olivary regions, and was sufficient to detect statistically significant differences in bouton sizes. The present data will thus benefit any future quantitative immunoelectron microscopic study.

Significance of particle analysis

Our observation that GAD immunostaining intensity is heterogeneous in the IO suggests that either the IO receives GABAergic innervation from several sources, which have boutons that are characteristically different and, therefore, produce regional variations in immunostaining intensity, or that anatomical or functional regional variations of the postsynaptic targets determine the heterogeneity of staining intensity (see Mugnaini 1970; Scheibel et al. 1956). A combination of these factors is also possible.

Papers in preparation demonstrate that at least three regions of the IO populated by GABAergic boutons of significantly different sizes receive GABAergic innervation from discrete sources. The beta nucleus contains the largest boutons, and is innervated by a GABAergic projection from the spinal vestibular nucleus (Nelson et al. 1986). Small GABAergic neurons in the lateral and interposed cerebellar nuclei project to subnuclei which contain the smallest GABAergic boutons in the IO; namely, the PO, the rostral lamella of the MAO, and the ventral lamella of the DAO (Nelson et al. 1984; Nelson and Mugnaini 1985; de Zeeuw et al. 1988). The dorsal fold of the DAO contains GABAergic boutons which are intermediate in size, and receives a GABAergic projection from the lateral vestibular nucleus (Nelson and Mugnaini 1988).

In conclusion, the present study demonstrates that GAD immunostaining patterns and individual bouton characteristics may be used as criteria for distinguishing olivary regions. In some regions, these parameters are correlated with particular GABAergic projections innervating the regions. A better understanding of the relationship between regional variations in GABAergic bouton characteristics and the distribution of different GABAergic projections may be derived from automated particle size analysis over large samples (now in progress) and the complete mapping of GABAergic afferents in the IO.

Acknowledgements. The authors wish to thank Dr. Albert Berrebi and Dr. Uwe Koehn for advice concerning the statistical analysis and Douglas E. Vetter for comments on the manuscript. This work was supported by USPHS Grant NS09904.

References

Andersson G, Hesslow G (1987a) Inferior olive excitability after high frequency climbing fibre activation in the cat. Exp Brain Res 67:523–532

Andersson G, Hesslow G (1987b) Activity of Purkinje cells and interpositus neurones during and after periods of high fre-

quency climbing fibre activation in the cat. Exp Brain Res 67:533–542
Azizi S, Woodward DJ (1987) Inferior olivary nuclear complex of the rat: morphology and comments on the principles of organization within the olivocerebellar system. J Comp Neurol 263:467–484
Barmack NH, Mugnaini E, Nelson B (1987) Vestibular modulation of the activity of inferior olivary neurons in the beta nucleus of the rabbit. Soc Neurosci [Abstr] 13:229
Bernard J-F (1987) Topographical organization of olivocerebellar and corticonuclear connections in the rat – an WGA-HRP study I. Lobules IX, X, and the flocculus. J Comp Neurol 263:241–258
Bloedel JR, Courville J (1981) Cerebellar afferent systems. In: Brooks VB (ed) Handbook of Physiology, vol II, 1. Motor Control. American Physiological Society, Bethesda MD, pp 735–829
Bowman JP, Sladek JR (1973) Morphology of the inferior olivary complex of the rhesus monkey (*Macacca mulatta*). J Comp Neurol 152:299–316
Brodal A (1940) Experimentelle Untersuchungen über die olivocerebellare Lokalisation. Z Ges Neurol Psychiatr 169:1–153
Brodal A (1976) The olivo-cerebellar projection in the cat as studied with the method of retrograde axonal transport of horseradish peroxidase II. The projection to the uvula. J Comp Neurol 166:417–426
Brodal A, Kawamura K (1980) Olivocerebellar projection: a review. Adv Anat Embryol Cell Biol 64:1–40
Brodal A, Walberg F (1977) The olivocerebellar projection in the cat studied with the method of retrograde transport of horseradish peroxidase IV. The projection to the anterior lobe. J Comp Neurol 172:85–108
Brodal P, Brodal A (1981) The olivocerebellar projection in the monkey. Experimental studies with the method of retrograde tracing of horseradish peroxidase. J Comp Neurol 201:375–393
Brown JT, Chan-Palay V, Palay S (1977) A study of afferent input to the inferior olivary complex in the rat by retrograde axonal transport of horseradish peroxidase. J Comp Neurol 176:1–22
Brown PA (1980) The inferior olivary connections to the cerebellum in the rat studied by retrograde axonal transport of horseradish peroxidase. Brain Res 5:267–275
Campbell NC, Armstrong DM (1983a) The olivocerebellar projection in the rat: an autoradiographic study. Brain Res 275:215–233
Campbell NC, Armstrong DM (1983b) Topographical localization in the olivocerebellar projection in the rat: an autoradiographic study. Brain Res 275:235–259
Courville J, Faraco-Cantin F (1978) On the origin of the climbing fibres of the cerebellum. An experimental study in the cat with an autoradiographic tracing method. Neuroscience 3:797–809
Desclin JC (1974) Histological evidence supporting the inferior olive as the major source of cerebellar climbing fibres in the rat. Brain Res 77:365–384
Eccles JC, Ito M, Szentágothai J (eds) (1967) The cerebellum as a Neuronal Machine. Springer, Berlin Heidelberg New York
Eisenman LM (1984) Organization of the olivocerebellar projection to the uvula in the rat. Brain Behav Evol 24:1–12
Furber SE, Watson CRR (1983) Organization of the olivocerebellar projection in the rat. Brain Behav Evol 22:132–152
Gotow T, Sotelo C (1987) Postnatal development of the inferior olivary complex in the rat: IV. Synaptogenesis of GABAergic afferents, analyzed by glutamic acid decarboxylase immunocytochemistry. J Comp Neurol 263:526–552
Groenewegen HJ, Voogd J (1977) The parasagittal zonation within the olivocerebellar projection: Climbing fiber distribution in the vermis of cat cerebellum. J Comp Neurol 174:417–488
Groenewegan HJ, Voogd J, Freedman SL (1979) The parasagittal zonal organization within the olivocerebellar projection. II. Climbing fiber distribution in the intermediate and hemispheric parts of cat cerebellum. J Comp Neurol 183:551–602
Gwyn DG, Nicholson GP, Flumerfelt BA (1977) The inferior olivary nucleus of the rat: a light and electron microscopic study. J Comp Neurol 174:489–520
Hoddevik GH, Brodal A, Walberg F (1976) The olivocerebellar projection in the cat studied with the method of retrograde axonal transport of horseradish peroxidase III. The projection to the vermal area. J Comp Neurol 169:155–170
Ito M (ed) (1984) The Cerebellum and Neural Control. Raven Press, New York
Krnjević K (1976) Inhibitory action of GABA and GABA-mimetics on vertebrate neurons. In: Roberts E, Chase TN, Tower DB (eds) GABA in Nervous System Function. Raven Press, New York, pp 269–281
Llinás R, Baker R, Sotelo C (1974) Electrotonic coupling between neurons in cat inferior olive. J Neurophysiol 37:560–571
Marani E (1986) Topographic histochemistry of the cerebellum. Prog Histochem Cytochem 16(4):1–161
Martin GF, Culberson J, Laxon C, Linauts M, Panneton M, Tschismadia I (1980) Afferent connections of the inferior olivary nucleus with preliminary notes on their development. Studies using the North American opossum. In: Courville J, de-Montigny C, Lamarre Y (eds) The Inferior Olivary Nucleus. Raven Press, New York, pp 35–72
McGrane MK, Woodward DJ, Eriksson MA, Burne RA, Saint-Cyr JA (1977) The inferior olivary complex in the rat: gross nuclear organization and topography of olivocerebellar projections. Soc Neurosci [Abstr] 3:59
McLaughlin BJ, Wood JG, Saito K, Barber R, Vaughn J-E, Roberts E, Wu J-Y (1974) The fine structural localization of glutamate decarboxylase in synaptic terminals of rodent cerebellum. Brain Res 76:377–391
Mugnaini E (1970) Neurones as synaptic targets. In: Andersen P, Jansen JKS (eds) Excitatory Synaptic Mechanisms. Universitetsforlaget, Oslo, pp 149–169
Mugnaini E, Dahl A-L (1983) Zinc-aldehyde fixation for light-microscopic immunocytochemistry of nervous tissue. J Histochem Cytochem 31:1435–1438
Mugnaini E, Oertel WH (1985) An atlas of the distribution of GABAergic neurons and terminals in the rat CNS as revealed by GAD immunohistochemistry. In: Björklund A, Hökfelt T (eds) Handbook of Chemical Neuroanatomy, vol 4. GABA and Neuropeptides in the CNS, part I. Elsevier Science Publishers, B.V., pp 436–608
Mugnaini E, Barmack NH, Oertel WH (1982) GABAergic innervation of the rabbit studied by GAD-immunocytochemistry. Soc Neurosci [Abstr] 8:445
Nelson B, Mugnaini E (1985) Loss of GABAergic nerve terminals in the inferior olive of cerebellectomized rats. Soc Neurosci [Abstr] 11:182
Nelson BJ, Mugnaini E (1988) Origins of GABAergic inputs to the inferior olive. In: Strata P (ed) The Olivocerebellar System in Motor Control (in press)
Nelson B, Barmack NH, Mugnaini E (1984) A GABAergic cerebello-olivary projection in the rat. Soc Neurosci [Abstr] 10:539
Nelson B, Barmack NH, Mugnaini E (1986) GABAergic projection from vestibular nuclei to rat inferior olive. Soc Neurosci [Abstr] 12:225
Oertel WH, Schmechel DE, Tappaz ML, Kopin IJ (1981a) Production of a specific antiserum to rat brain glutamic acid decarboxylase by injection of an antigen-antibody complex. Neuroscience 6:2689–2700
Oertel WH, Schmechel DE, Mugnaini E, Tappaz ML, Kopin IJ (1981b) Immunocytochemical localization of glutamate decarboxylase in rat cerebellum with a new antiserum. Neuroscience 6:2715–2735
Oertel WH, Mugnaini E, Schmechel DE, Tappaz ML, Kopin IJ (1982) The immunocytochemical demonstration of GABAergic neurons – methods and application. In: Chan-Palay V, Palay SL (eds) Cytochemical Methods in Neuroanatomy. Alan R Liss, New York, pp 279–329
Oertel WH, Schmechel DE, Mugnaini E (1983) Glutamic acid decarboxylase (GAD): purification, antiserum production, im-

munocytochemistry. In: Barker JL, McKelvy JF (eds) Current Methods in Cellular Neurobiology. John Wiley and Sons, New York, pp 63–110

Ordronneau P, Lindstrom PB-M, Petrusz P (1981) Four unlabelled antibody bridge techniques. J Histochem Cytochem 29:1397–1404

Ottersen OP, Storm-Mathisen J (1984) Glutamate- and GABA-containing neurons in the mouse and rat brain, as demonstrated with a new immunocytochemical technique. J Comp Neurol 229:374–392

Ottersen OP, Storm-Mathisen J (1987) Localization of amino acid neurotransmitters by immunocytochemistry. TINS 10:250–255

Paré M, Descarries L, Wiklund L (1987) Innervation and reinnervation of rat inferior olive by neurons containing serotonin and substance P: an immunohistochemical study after 5,6-dihydroxytryptamine lesioning. J Neurocytol 16:155–167

Roberts E (1979) New directions in GABA research I: Immunocytochemical studies of GABA neurons. In: Krogsgaard-Larsen P, Scheel-Krüger J, Kofod H (eds) GABA-Neurotransmitters: Pharmaco-chemical, Biochemical and Pharmacological Aspects. Proceeding, Alfred Benzon Symposium 12:28–45. Munksgaard Copenhagen

Saito K, Barber R, Wu J-Y, Matsuda T, Roberts E, Vaughn JE (1974) Immunohistochemical localization of glutamic acid decarboxylase in rat cerebellum. PNAS, USA 71:269–273

Sasaki K, Llinás R (1985) Evidence for dynamic electrotonic coupling in mammalian inferior olive in vivo. Soc Neurosci [Abstr] 11:181

Scheibel M, Scheibel A, Walberg F, Brodal A (1956) Areal distribution of axonal and dendritic patterns in inferior olive. J Comp Neurol 106:21–47

Sotelo C, Gotow T, Wassef M (1986) Localization of glutamic-acid-decarboxylase-immunoreactive axon terminals in the inferior olive of the rat, with special emphasis on anatomical relations between GABAergic synapses and dendro-dendritic gap junctions. J Comp Neurol 252:32–50

Spira ME, Bennett MVL (1972) Synaptic control of electrotonic coupling between neurons. Brain Res 37:294–300

Spira ME, Spray DC, Bennett MVL (1980) Synaptic organization of expansion motoneurons of *Navanax inermis*. Brain Res 195:241–269

Swenson RS, Castro AJ (1983) The afferent connections of the inferior olivary complex in rats. An anterograde study using autoradiographic and axonal degeneration techniques. Neuroscience 8:259–275

Szentágothai J, Rajkovitz K (1959) Über den Ursprung der Klatterfasern des Kleinhirns. Z Anat Entwickl Gesch 121:130–141

Takahashi TT, Carr CE, Brecha N, Konishi M (1987) Calcium binding protein-like immunoreactivity labels the terminal field of nucleus laminaris of the barn owl. J Neuroscience 7:1843–1856

Voogd J, Bigaré F (1980) Topographical distribution of olivary and corticonuclear fibers in the cerebellum. A review. In: Courville J, de Montigny C, Lamarre Y (eds) The Inferior Olivary Nucleus. Raven Press, New York, pp 207–234

Walberg F (1956) Descending connections to the inferior olive. J Comp Neurol 104:77–174

Walberg F (1960) Further studies on the descending connections to the inferior olive: reticulo-olivary fibers. J Comp Neurol 114:79–87

Whitworth RH, Haines DE (1986) On the question of nomenclature of homologous subdivisions of the inferior olivary complex. Arch Ital Biol 124:271–317

Wiklund L, Toggenburger G, Cuenod M (1984) Selective retrograde labelling of the rat olivocerebellar climbing fiber system with D-(^{3}H)Aspartate. Neuroscience 13:441–468

Wood JG, McLaughlin BJ, Vaughn JE (1976) Immunocytochemical localization of GAD in electron microscopic preparation of rodent CNS. In: Roberts E, Chase TN, Tower DB (eds) GABA in Nervous System Function. Raven Press, New York, pp 133–148

Wu J-Y (1976) Purification, characterization and kinetic studies of GAD and GABA-T from mouse brain. In: Roberts E, Chase TN, Tower DB (eds) GABA in Nervous System Function. Raven Press, New York, pp 7–55

Wu J-Y, Matsuda T, Roberts E (1973) Purification and characterization of glutamate decarboxylase from mouse brain. J Biol Chem 248:3029–3034

deZeeuw CI, Holstege JC, Calkoen F, Ruigrok TJH, Voogd J (1988) A new combination of WGA-HRP anterograde tracing and GABA immunocytochemistry applied to afferents of the cat inferior olive at the ultrastructural level. Brain Res 447:369–375

Accepted August 5, 1988